

RESEARCH

Open Access



Feedback control of heart rate during robotics-assisted tilt table exercise in patients after stroke: a clinical feasibility study

Lars Brockmann¹, Jittima Saengsuwan^{1,2}, Corina Schuster-Amft^{1,3,4} and Kenneth J. Hunt^{1*} 

Abstract

Background Patients with neurological disorders including stroke use rehabilitation to improve cognitive abilities, to regain motor function and to reduce the risk of further complications. Robotics-assisted tilt table technology has been developed to provide early mobilisation and to automate therapy involving the lower limbs. The aim of this study was to evaluate the feasibility of employing a feedback control system for heart rate (HR) during robotics-assisted tilt table exercise in patients after a stroke.

Methods This feasibility study was designed as a case series with 12 patients ($n = 12$) with no restriction on the time post-stroke or on the degree of post-stroke impairment severity. A robotics-assisted tilt table was augmented with force sensors, a work rate estimation algorithm, and a biofeedback screen that facilitated volitional control of a target work rate. Dynamic models of HR response to changes in target work rate were estimated in system identification tests; nominal models were used to calculate the parameters of feedback controllers designed to give a specified closed-loop bandwidth; and the accuracy of HR control was assessed quantitatively in feedback control tests.

Results Feedback control tests were successfully conducted in all 12 patients. Dynamic models of heart rate response to imposed work rate were estimated with a mean root-mean-square (RMS) model error of 2.16 beats per minute (bpm), while highly accurate feedback control of heart rate was achieved with a mean RMS tracking error (RMSE) of 2.00 bpm. Control accuracy, i.e. RMSE, was found to be strongly correlated with the magnitude of heart rate variability (HRV): patients with a low magnitude of HRV had low RMSE, i.e. more accurate HR control performance, and *vice versa*.

Conclusions Feedback control of heart rate during robotics-assisted tilt table exercise was found to be feasible. Future work should investigate robustness aspects of the feedback control system. Modifications to the exercise modality, or alternative modalities, should be explored that allow higher levels of work rate and heart rate intensity to be achieved.

Keywords Heart rate dynamics, Heart rate control, Feedback control, Stroke, Neurorehabilitation, Rehabilitation robotics

*Correspondence:

Kenneth J. Hunt

kenneth.hunt@bfh.ch

Full list of author information is available at the end of the article



© The Author(s) 2024. **Open Access** This article is licensed under a Creative Commons Attribution-NonCommercial-NoDerivatives 4.0 International License, which permits any non-commercial use, sharing, distribution and reproduction in any medium or format, as long as you give appropriate credit to the original author(s) and the source, provide a link to the Creative Commons licence, and indicate if you modified the licensed material. You do not have permission under this licence to share adapted material derived from this article or parts of it. The images or other third party material in this article are included in the article's Creative Commons licence, unless indicated otherwise in a credit line to the material. If material is not included in the article's Creative Commons licence and your intended use is not permitted by statutory regulation or exceeds the permitted use, you will need to obtain permission directly from the copyright holder. To view a copy of this licence, visit <http://creativecommons.org/licenses/by-nc-nd/4.0/>.

Background

Patients with neurological disorders such as spinal cord injury (SCI) or stroke, and patients with acquired brain injury (ABI), use rehabilitation to improve cognitive abilities, to regain motor function and to reduce the risk of further complications. One complication that can arise from prolonged bed rest or reduced mobility is orthostatic hypotension (OH). OH is a physical condition where a person's blood pressure drops considerably (systolic blood pressure decrease of at least 20 mmHg or diastolic blood pressure decrease of at least 10 mmHg) within three minutes of standing [1].

A common form of treatment for such patients is verticalisation with the help of tilt tables and passive movement of the lower extremities [2]. Robotic rehabilitation devices have been developed and deployed clinically to assist in performing such therapies. The Erigo (Hocoma AG, Switzerland) is one example. It is a robotics-assisted tilt table suited to the early stages of rehabilitation that allows for progressive verticalisation up to 90° with the addition of an integrated, motorised stepping function to simulate gait [3]. The Erigo's stepping function is essentially passive: the lower extremities are mobilised by mechanically shifting the thighs back and forth without active patient participation, although the latest edition of the device includes a functional electrical stimulation (FES) module for activation of paralysed muscle.

On these grounds, our previous work adapted the Erigo by implementing a real-time visual feedback system and force sensors in the thigh cuffs to allow work rate estimation [4]. This enables patients with at least partially retained motor function to actively participate in the rehabilitation exercise through volitional effort. Patients can adapt their leg forces to keep to a target work-rate profile displayed on the biofeedback screen. Studies involving mild-to-severe stroke impairment [5, 6] and spinal cord injury [7] established that meaningful physiological responses could be developed and formal exercise tests could be performed reliably while exercising using this modality. Furthermore, a pilot study, conducting experiments on four healthy participants, developed and successfully tested a method for automatic control of heart rate using this device [4].

A related approach to heart rate control using the Erigo, albeit using only stepping frequency and tilt angle to drive the exercise, and using only six healthy participants, has also been proposed [8]. Because of the employment of only the standard device settings, and the lack of any biofeedback that facilitated active participation to increase work rate, participants remained passive and the magnitude of increase in heart rate was very limited, being only 9 beats/min above resting levels.

Integrating automatic heart rate control algorithms into rehabilitation platforms, such as the Erigo, could enhance prescription and monitoring of patients' physiological responses while exercising, thereby contributing to a safer rehabilitation process with desired target heart rate intensities being achieved more accurately. It is important to use feedback to control heart rate intensity directly because a given force or work rate will lead to potentially very different heart rates in different patients: but with feedback, the compensator will, in principle, automatically find the correct and individual force or work rate that will lead to the target heart rate being reached.

Exercise with integrated heart rate control is expected to ensure active patient participation as the patient has to continuously adapt their output work rate to match the changing target. Active patient participation is presumed to improve therapeutic efficacy [9]. The use of heart rate as a proxy of exercise intensity has been extensively described for healthy able-bodied people and for patients with a very wide range of disease and impairment conditions [10]. The latter reference includes specific guidelines for using HR in exercise testing and prescription and provides an extensive collection of background literature citations.

Before the putative benefits of integrating automatic heart rate control algorithms into clinical rehabilitation can be realised, the technical feasibility of this proposal must first be demonstrated. The present work therefore aimed to evaluate the technical feasibility of employing a feedback control system for heart rate during robotics-assisted tilt table exercise in a clinical case series of patients after a stroke.

Methods

Study design and patients

This feasibility study was designed as a case series with 12 patients ($n = 12$). The study was conducted at Reha Rheinfelden, a specialised neurorehabilitation clinic in the northeast region of Switzerland. Eligible patients were recruited from the inpatient population, from those attending the clinic's neurological daycare centre (NDC) and from outpatients. The sample size of $n = 12$ was specified *a priori* in the approved study protocol based on recommendations regarding the conduct of feasibility trials [11].

Inclusion criteria were: a diagnosis of first-ever stroke; age > 18 years; clinical stability; the ability to communicate well, sustain attention and follow instructions; and the capacity of judgement. All degrees of post-stroke impairment severity were allowed and there was no restriction on the time post-stroke. The principal exclusion criteria were severe cognitive impairment, a history

of cardiovascular or pulmonary disease that may have presented risk or abnormal physiological responses during exercise, medications that may have influenced heart rate response to exercise (e.g. beta blockers), or patients with contraindications for the robotics-assisted tilt table according to the manufacturer's instructions.

The study was reviewed and approved by the Ethics Committee of Northwestern and Central Switzerland (EKNZ, Ref. 2022-01935). Patients provided written, informed consent prior to inclusion in the study.

Equipment

All exercises were performed on a robotics-assisted tilt table (Erigo, Hocoma AG, Switzerland; Fig. 1). The tilting mechanism provides verticalisation up to 90° while the drives allow stepping-like motion at a rate of up to 80 steps/min. The device includes a body harness and leg cuffs that are attached to the thighs just above the knee (Fig. 1a). Force sensors were integrated into the leg cuffs to allow volitional patient effort to be measured; leg force together with angular motion allowed total volitional work rate (WR) to be estimated as the product of force, lever arm and angular velocity, summed over the two legs. This estimated WR is referred to in the following as "actual" work rate in contradistinction to the target work rate.

A biofeedback monitor was positioned in front of the tilt table (Fig. 1b) to display a target work rate (WR*) and the actual work rate (WR); during active exercise, patients were instructed to focus on the display and to continuously adjust their volitional leg force to keep their work rate as close as possible to the target.

Heart rate (HR) was monitored using a chest-belt sensor (H10, Polar Oy, Finland) and transmitted wirelessly to a custom control application implemented in Matlab/Simulink (The MathWorks, Inc., USA) running in real time on a PC. This heart rate monitor also delivered raw RR intervals for separate analysis of heart rate variability (HRV). Blood pressure was monitored periodically during each test to ensure patient safety. The overall experimental setup is illustrated in Figs. 2 and 3.

Test procedures and outcome measures

Each patient took part in two test sessions, with each test session separated by at least 24 h. The first session had a planned duration of 70 min to 90 min and comprised a familiarisation with the Erigo and the measurement instruments, followed by a formal system identification test. The second session was a formal heart rate control test with a planned duration of about 60 min. Patients were instructed to avoid strenuous activity within the 24 h before testing and not to consume caffeine at least



(a) Front view showing body harness and leg cuffs.



(b) Rear view showing biofeedback screen.

Fig. 1 Erigo robotics-assisted tilt table

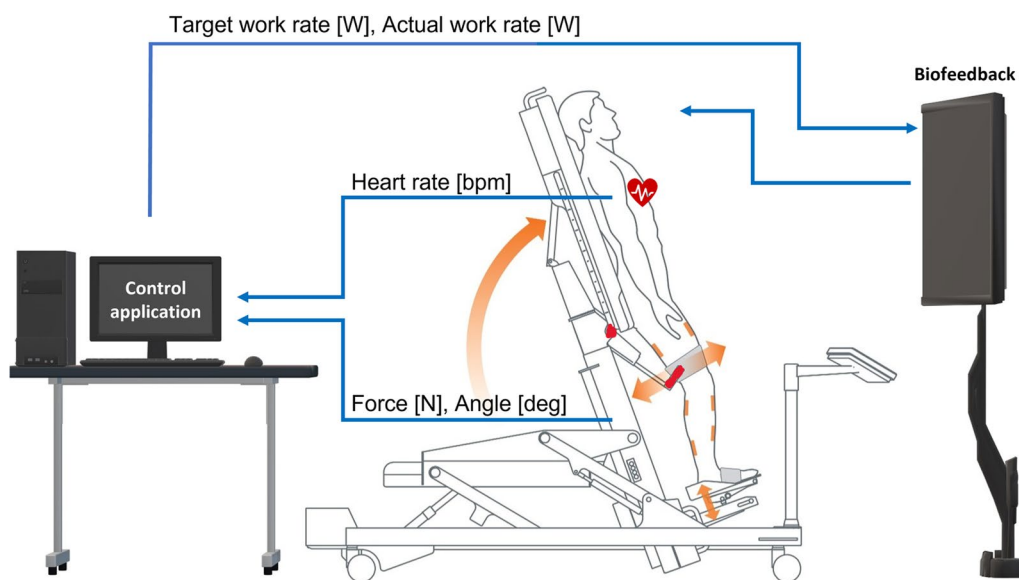


Fig. 2 Experimental setup—schematic. The control application continuously displays a target work rate, WR^* , on the biofeedback screen along with the actual work rate, WR . The latter is estimated from measured forces and angles. The locations of the force and position sensors are indicated with a red bar just below the thigh cuff and a red dot close to the hip joint, respectively. Heart rate is also recorded in real time

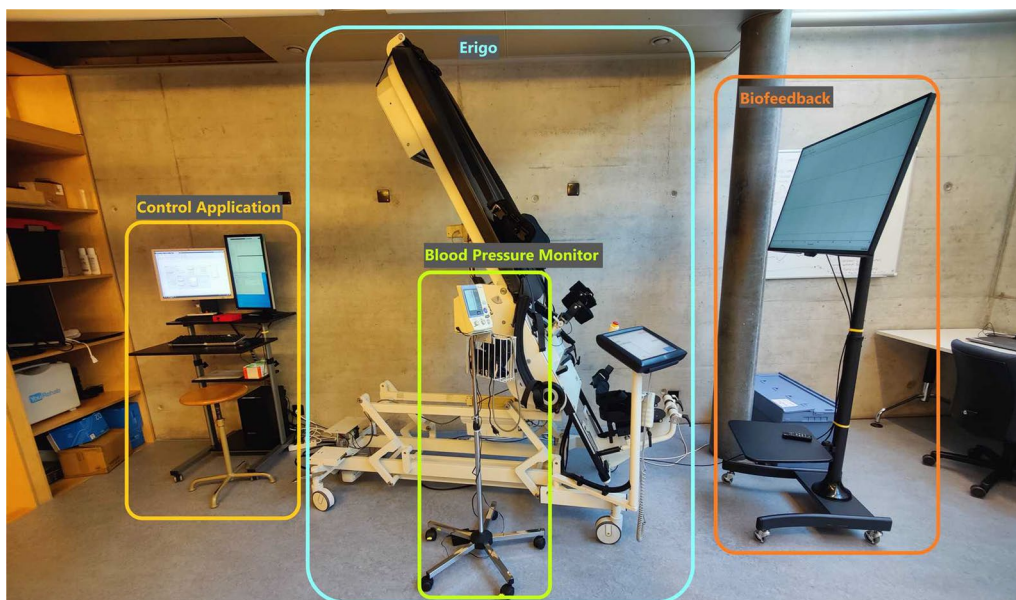


Fig. 3 Experimental setup—in situ

3 h prior to testing. In all tests, the tilt angle was set to 60° and the stepping cadence to the maximum of 80 steps/min.

System identification

In the system identification tests, which are open-loop tests as far as heart rate is concerned, the target work rate WR^* was defined as two periods of a square wave

of period 6 min, with the two levels, WR_1^* and WR_2^* , set within the light-to-moderate exercise intensity range (Fig. 4). The specific work-rate levels were determined for each patient individually by evaluating the work rates applied and heart rate responses observed during the preceding familiarisation session.

Identification tests began with 3 min of passive movement where the patient was instructed to relax while

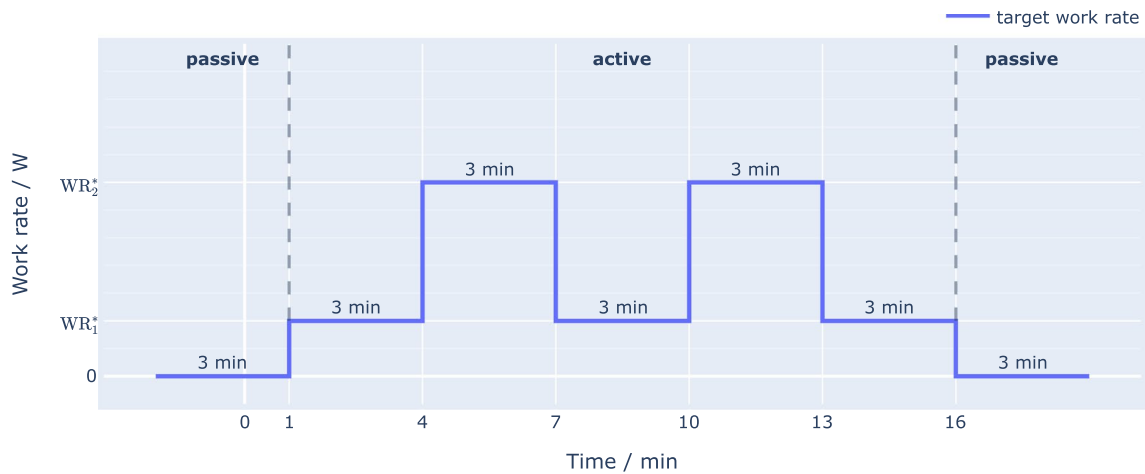


Fig. 4 Target work rate profile for system identification

their legs were moved by the device. During the 15-min active phase, the patient was instructed to follow as closely as possible the square-wave target work rate displayed on the screen along with their measured work rate. The test concluded with a 3-min passive phase. HR was recorded for further analysis.

Heart rate response to changes in target work rate, considered mathematically as a mapping from WR^* to HR, were modelled as the first-order, linear time-invariant (LTI) transfer function

$$P_o(s) = \frac{k}{\tau s + 1}: WR^* \mapsto HR \tag{1}$$

where the model (also referred to as the open-loop plant) is parameterised by a steady-state gain k and a time constant τ ; the units of k and τ are beats per minute (bpm) per Watt (bpm/W) and seconds, respectively; s is the Laplace transform complex variable. The purpose of the system identification procedure was to estimate these parameters empirically using the test data; a separate model was identified for each individual patient. We employed a least-squares optimisation algorithm (function procest) from the Matlab System Identification Toolbox (The MathWorks, Inc., USA), which is the standard method recommended for LTI models of the form Eq. (1), [12]. Several previous studies of HR control with able-bodied participants and using cycle ergometer or treadmill exercise modalities, e.g. [13], have demonstrated that a linear time-invariant model such as Eq. (1) leads to accurate and robust HR control performance, thus providing the basis for this choice of model in the present study.

The goodness of fit of the estimated models was quantified using a normalised root-mean-square model

error (NRMSE), also called “fit”, and the absolute RMS model error (RMSE_I, where “I” denotes Identification):

$$\text{fit (NRMSE) [I]} = \left(1 - \frac{\sum_{i=1}^N (HR(i) - HR_{sim}(i))^2}{\sum_{i=1}^N (HR(i) - \overline{HR})^2} \right) \times 100 \%, \tag{2}$$

$$\text{RMSE}_I \text{ [bpm]} = \sqrt{\frac{1}{N} \sum_{i=1}^N (HR_{sim}(i) - HR(i))^2}. \tag{3}$$

In the above, HR is the measured heart rate, \overline{HR} is the mean heart rate, and HR_{sim} is the heart rate that was simulated using the estimated models. The summations range over the evaluation period up to the number of data points included, N . The square brackets, [·], indicate the units for these quantities.

Feedback control

In the feedback control tests, which are closed-loop tests as far as heart rate is concerned, the target heart rate HR^* was set to a constant level within the light-to-moderate exercise intensity range for a duration of up to 20 min (Fig. 5). The target HR level was determined for each patient individually by evaluating the HR values measured during the system identification test, and initially setting HR^* within the observed range. In practice, it was found necessary in 6 of 12 cases to adjust HR^* manually during the first few minutes of the active phase of the feedback control tests to ensure patients could maintain the target and/or to keep the exercise intensity within the desired range. This is likely due to fatigue or other factors

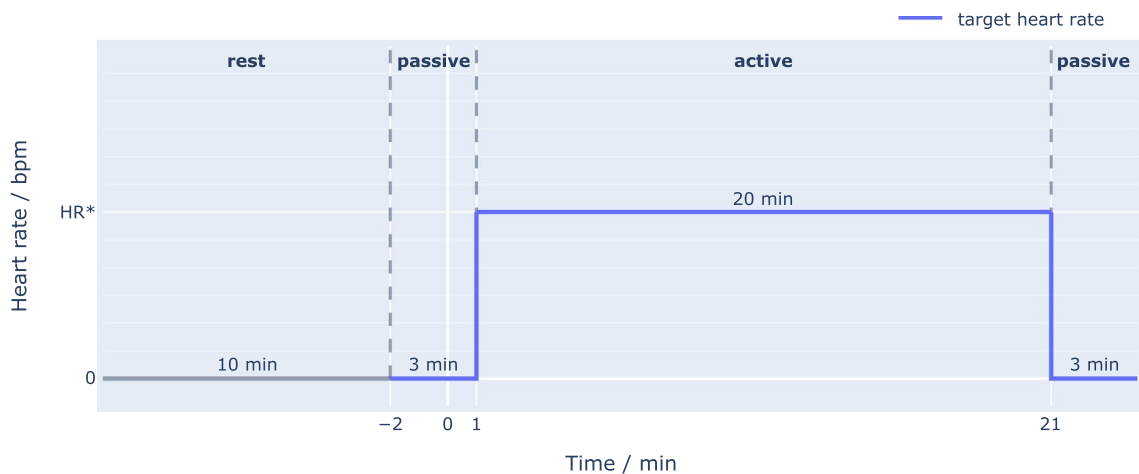


Fig. 5 Target heart rate profile for feedback control

that affected patients’ performance. The 20-min active phase of exercise was preceded and followed by 3-min passive phases (Fig. 5).

Automatic control of heart rate was implemented using a classical feedback control structure (Fig. 6; [14]). Measured heart rate HR (generic variable y) is fed back and compared to the target value HR^* (generically, r) to obtain the tracking error e . The error is processed by the dynamic compensator [transfer function $C(s)$] that continuously adjusts the manipulated variable, also known as the control signal, that is to say the target work rate WR^* (u) displayed to the patient, to minimise the error term. Variations in WR^* then result in a measured HR that depends on the dynamic plant transfer function $P_o(s)$, Eq. (1). The term d represents the lumped effect of disturbances that influence the heart rate, which principally comprises heart rate variability (HRV), [15].

The feedback compensator $C(s)$ was designed with the aim of making the manipulated variable (target heart rate WR^* , generic signal u) relatively insensitive to the HRV disturbance term d . To this end, we employed an input-sensitivity loop-shaping approach that is described in detail elsewhere, [15], and summarised here. For the generic feedback loop, Fig. 6, the transfer function linking the input signals r and d to the manipulated variable

u is known as the input sensitivity function, and it is given by (see ref. [14])

$$U_o(s) = \frac{C(s)}{1 + C(s)P_o(s)}: r, d \mapsto u. \tag{4}$$

To make the magnitude of this function well behaved, that is to say, to make it free of peaking and to roll off at high frequency, it is constrained to take the form of a first-order transfer function with a specified bandwidth p , viz.

$$U_o(s) = \frac{p/k}{s + p}: r, d \mapsto u. \tag{5}$$

The factor $1/k$, i.e. the inverse of the plant steady-state gain, appears by virtue of the compensator being constrained to have integral action (factor $1/s$ in $C(s)$; see Eq. (6), below) and therefore infinite steady-state gain; under this condition, $U_o(0)$ in Eq. (4) is seen to equal $1/P(0)$ which, from Eq. (1), is equal to $1/k$.

The feedback compensator $C(s)$ that meets the above design goal can be derived in the following steps (this is a summary of the full derivation that can be found in [15]). In their generic rational forms, the plant and compensator transfer functions are denoted as $P_o = B/A$ and $C = G/H$ where A, B, G and H are polynomials in

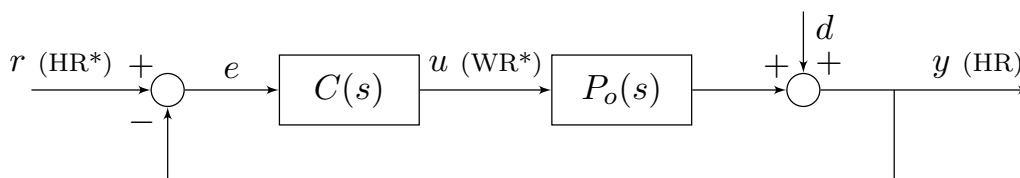


Fig. 6 Structure of feedback control loop. The generic variables r, y and u represent, respectively, target heart rate HR^* , measured heart rate HR, and target work rate WR^* , as indicated

s. From Eq. (1), $A = s + 1/\tau$ and $B = k/\tau$; it remains to determine G and H .

The classical closed-loop characteristic equation, [14], is $\Phi = AH + BG$. To achieve the design goals, the compensator is constrained to cancel plant poles and to include integral action by setting $G = g_0A$ and $H = sH'$, with g_0 a constant. The characteristic equation is then $\Phi = AsH' + Bg_0A$ which implies that A must be a factor of Φ , viz. $\Phi = A\Phi'$, giving $\Phi' = sH' + Bg_0$. Substituting in the generic expression for U_o , Eq. (4), gives $U_o = g_0A/\Phi'$. To further simplify U_o down to a first-order transfer function as desired, we set $\Phi' = A(s + p)$ to get $U_o = g_0/(s + p)$ which is exactly the form we set out to achieve: cf. Eq. (5).

Regarding stability, we note that the closed-loop characteristic polynomial Φ has the form $\Phi = A\Phi' = A^2(s + p)$. Nominal closed-loop stability is thus guaranteed by virtue of stable A (the open-loop plant is stable) and choice of the design parameter p as a positive number.

Finally, the controller parameters are obtained by explicit solution of the reduced characteristic equation $sH' + g_0k/\tau = A(s + p) = (s + 1/\tau)(s + p)$, giving $g_0 = p/k$ and $H' = s + p + 1/\tau$.

For the nominal plant Eq. (1), the compensator that results in the desired form for the input sensitivity function, viz. Eq. (5), is thus given by

$$C(s) = \frac{g_0A}{sH'} = \frac{\frac{p}{k}\left(s + \frac{1}{\tau}\right)}{s\left(s + p + \frac{1}{\tau}\right)}: e \mapsto u. \quad (6)$$

This expression is seen to have a very simple form: its parameters depend only upon the empirically-determined plant gain k and time constant τ obtained from system identification, and on the desired closed-loop bandwidth p which can be freely chosen to adjust the control performance. For all of the feedback control tests performed in this study, the bandwidth was set to $f = 0.01$ Hz, or $p = 2\pi f = 0.0628$ rad/s.

In summary, model parameters k and τ were estimated individually for each patient using data from the system identification tests, and feedback compensators were calculated individually for each patient using the expression Eq. (6) with bandwidth $p = 0.0628$ rad/s.

In the feedback control tests, the accuracy of heart rate control was quantified using the difference between the actual HR response and the nominal HR as the root-mean-square tracking error (RMSE_C, where "C" denotes Control)

$$\text{RMSE}_C [\text{bpm}] = \sqrt{\frac{1}{N} \sum_{i=1}^N (\text{HR}_{\text{sim}}(i) - \text{HR}(i))^2}, \quad (7)$$

where HR_{sim} is the nominal closed-loop heart rate response obtained by simulating the feedback loop (Fig. 6) with individual compensator and plant parameters, and with $d = 0$.

To obtain a measure of the intensity of changes in the manipulated variable u (i.e. target work rate WR^*), we used the average power of changes in the control signal, viz.

$$P_{\nabla u} [\text{W}^2] = \frac{1}{N-1} \sum_{i=2}^N (u(i) - u(i-1))^2. \quad (8)$$

This outcome is important because it quantifies how dynamic the control signal is. Since the control signal in this application is the target work rate WR^* that is presented to the patient, it is important that control signal power is low in a relative sense so that the patient can follow this target as accurately as possible.

In a similar vein to evaluation of HR tracking accuracy, the accuracy of patients' volitional work rate control was quantified using an RMS error, RMSE_{WR} , defined as

$$\text{RMSE}_{\text{WR}} [\text{W}] = \sqrt{\frac{1}{N} \sum_{i=1}^N (\text{WR}^*(i) - \text{WR}(i))^2}. \quad (9)$$

The summations in Eqs. (7), (8) and (9) range over the evaluation period up to the number of data points included, N .

Results

All 12 patients completed the two test sessions: there were no dropouts.

Study cohort

The study population of 12 patients had ages from 32 years to 77 years, NIHSS scores ranging from 1 to 11, and FAC scores from 1 to 5 (Table 1). Seven patients were inpatients, three were from the daycare centre, and two were outpatients (summary, along with additional relevant parameters, in Table 2).

System identification

The estimated steady-state gains and time constants varied quite widely: k was on the range 0.55 bpm/W to 3.00 bpm/W and τ ranged from 24.5 s to 79.0 s (Table 3); mean RMS model error RMSE_1 was 2.16 bpm and mean fit was 44.7 %. Despite the wide dispersion of k and τ , the average of all 12 models had quite narrow bounds [95 % confidence intervals (CIs)] for the mean values of

Table 1 Individual patient data, $n = 12$

ID	Sex	Age [years]	Height [cm]	Mass [kg]	BMI [kg/m ²]	NIHSS	MRS	FAC
1	f	72	1.68	68.0	24.1	6	3	3
2	m	62	1.87	103.0	29.5	2	1	5
3	f	41	1.63	60.0	22.6	8	4	2
4	f	75	1.51	92.0	40.3	2	1	5
5	f	77	1.55	67.0	27.9	2	1	5
6	m	41	1.75	66.7	21.8	1	1	5
7	m	56	1.74	95.0	31.4	5	4	1
8	f	33	1.65	58.0	21.3	2	1	5
9	m	32	1.83	79.0	23.6	3	2	5
10	f	57	1.68	68.0	24.1	2	1	5
11	f	60	1.68	63.0	22.3	11	3	2
12	m	57	1.76	118.0	38.1	1	1	5
Mean (SD)		55.2 (15.6)	169.4 (10.5)	78.1 (19.3)	27.2 (6.4)	3.8 (3.1)	1.9 (1.2)	4.0 (1.5)

ID: patient identification number; BMI: Body mass index; NIHSS: National Institutes of Health Stroke Scale; MRS; Modified Rankin Scale; FAC: Functional Ambulation Category; f: female; m: male; SD: standard deviation

Table 2 Summary patient data, $n = 12$

Clinical data	
Days since stroke	Inpatients: 50 days (mean, $n = 7$) NDC patients: 391 days (mean, $n = 3$) Outpatients: 1425 days (mean, $n = 2$)
Type of stroke	Ischaemic (10/12), Haemorrhagic (2/12)
Hemiparetic side	Left (7/12), Right (4/12), n/a (1/12).
NIHSS	0 (0/12), 1 (2/12), 2 (5/12), 3 (1/12), 4 (0/12), 5 (1/12), 6 (1/12), 7 (0/12), 8 (1/12), 9 (0/12), 10 (0/12), 11 (1/12), 12–42 (0/12)
MRS	0 (0/12), 1 (7/12), 2 (1/12), 3 (2/12), 4 (2/12), 5 (0/12), 6 (n/a)
FAC	0 (0/12), 1 (1/12), 2 (2/12), 3 (1/12), 4 (0/12), 5 (8/12)

NDC: Neurological Daycare Centre; NIHSS: National Institutes of Health Stroke Scale; MRS: Modified Rankin Scale; FAC: Functional Ambulation Category

Table 3 Estimated model parameters and goodness-of-fit

ID	k [bpm/W]	τ [s]	RMSE _E [bpm]	fit [%]
1	2.32	51.6	1.94	57.6
2	0.62	25.7	1.70	49.4
3	1.42	62.8	1.49	47.4
4	2.14	42.0	1.54	63.4
5	0.91	43.1	1.13	43.3
6	0.81	26.4	2.49	44.0
7 ^a	1.40	42.0	3.87	16.9
8	1.98	24.5	2.88	45.0
9	0.74	39.9	1.73	36.4
10 ^b	3.00	79.0	4.59	45.0
11	1.35	40.2	1.36	44.2
12	0.55	66.4	1.14	43.5
Mean \pm SD	1.44 \pm 0.78	45.3 \pm 17.0	2.16 \pm 1.11	44.7 \pm 11.2

ID: patient identification number; SD: standard deviation

^a Model parameters set to average of ID 1–6

^b Gain manually set to empirical estimate

$k = 1.44$ bpm/W, 95 % CI 0.94 bpm/W to 1.93 bpm/W, and $\tau = 45.3$ s, 95 % CI 34.5 s to 56.1 s (Fig. 7). Furthermore, using a Kolmogorov-Smirnov test with Lilliefors correction, the sample distributions of k and τ were found to be not significantly different from normality ($p = 0.37$ for k , $p = 0.12$ for τ).

For patients 7 and 10, the optimisation algorithm failed to compute realistic model parameters, likely due to poor data quality from the corresponding identification experiments. Patient 7 had difficulty maintaining the target work rate during the identification test. This resulted in variations in heart rate that were not attributable to the square-wave work rate target alone. Patient 10 did manage to accurately follow the target work rate during the identification test but, for reasons unknown, the heart rate displayed substantial and apparently random fluctuations.

Consequently, the parameters for patient 7 were set to the average values of the previous models (ID 1–6). For

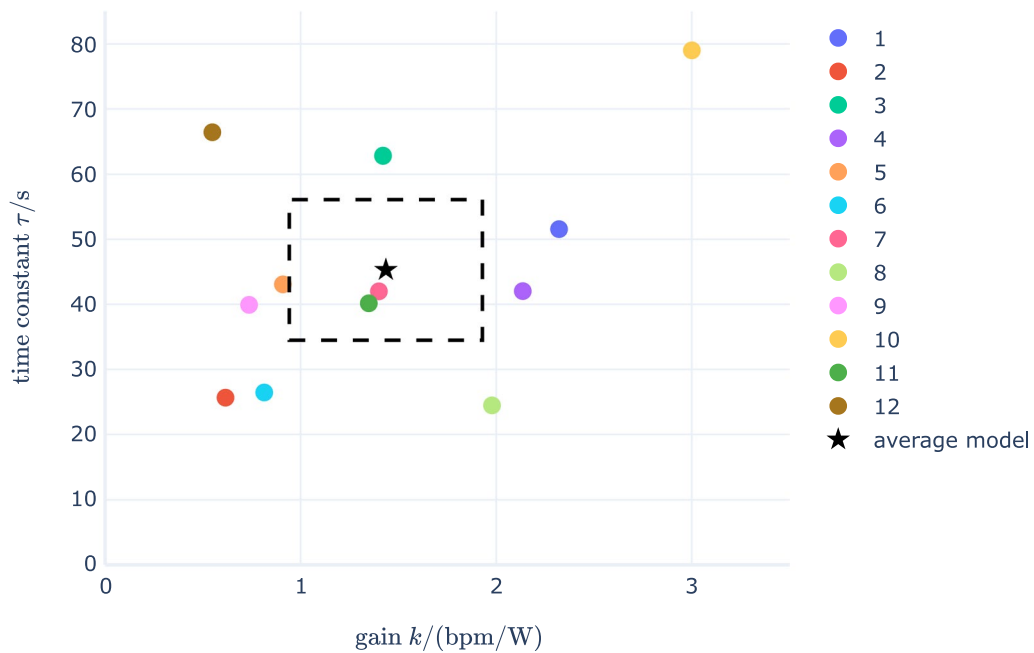


Fig. 7 Dispersion of individually-estimated model parameters. The star denotes the average of all models and the dashed box bounds the 95 % confidence intervals for the mean $k = 1.44$ bpm/W (95 % CI 0.94 bpm/W to 1.93 bpm/W) and $\tau = 45.3$ s (95 % CI 34.5 s to 56.1 s). The legend on the right-hand side indicates individual patient identification numbers

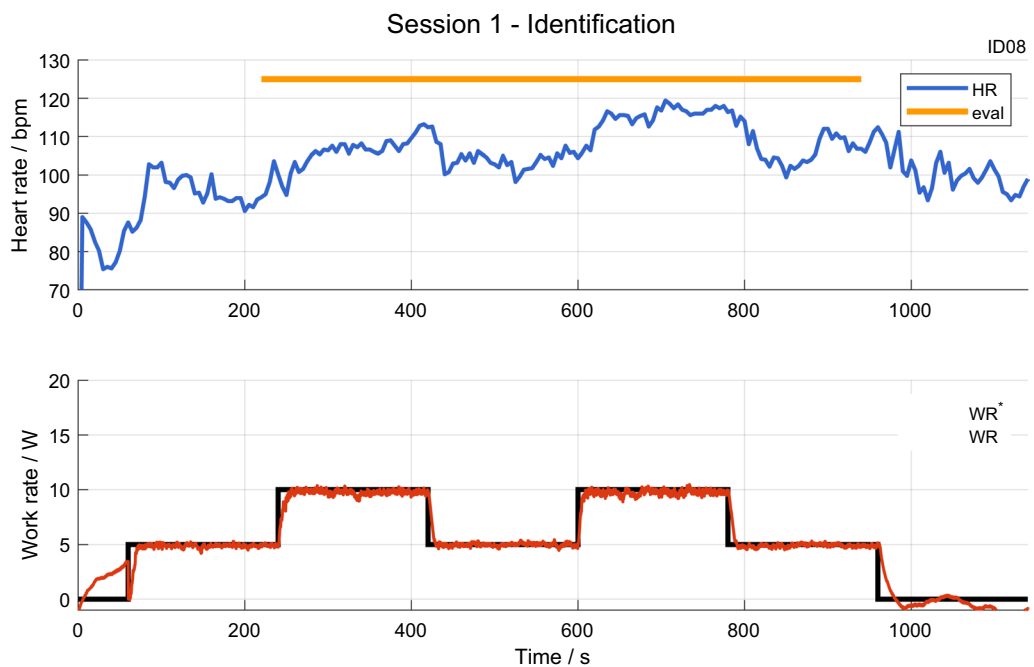


Fig. 8 Raw data from system identification test for patient 8. The lower plot shows the target (WR^* , black) and actual (WR, red) work rates. The upper plot shows the measured HR. The orange bar signifies the time period used for parameter estimation and model validation

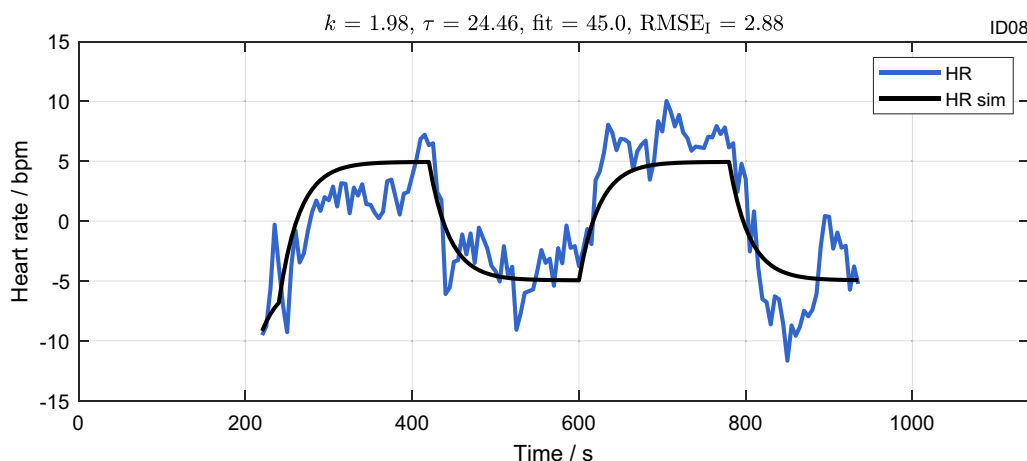


Fig. 9 Validation of estimated model for patient 8. The measured HR data are plotted alongside the model-simulated HR

patient 10, k was manually constrained by visual inspection of this patient’s step responses to the value 3 bpm/W, and τ was then estimated by the optimisation algorithm.

For illustration, an exemplary data set from the system identification tests is provided: this shows the raw data (Fig. 8) and validation of the estimated model by quantitative comparison of measured and simulated outputs (Fig. 9). These data are from patient 8, chosen because the fit of 45.0 % is closest to the mean fit for all patients (Table 3). It is evident from the lower plot in Fig. 8 that this patient was able to follow the target work rate very precisely by continuous modification of their volitional effort.

Feedback control

Feedback control tests were successfully conducted in all 12 patients, albeit the test with patient 7 was terminated quite early (after approximately 5 min) due to their inability to produce and sustain the target work rate. On average, the target heart rate was set to 94 bpm; this corresponds to 57 % of the average age-predicted maximal heart rate of 220 - age, which in turn lies within the “light” exercise intensity range as defined by the American College of Sports Medicine [10].

Overall, HR tracking accuracy was very good, with a mean root-mean-square tracking error $RMSE_C$ of 2.00 bpm (Table 4). The range of $RMSE_C$ was 0.97 bpm to 4.43 bpm, whereby 9 of the 12 tests had an $RMSE_C$ of less than 2 bpm. The mean value of average control signal power P_{Vu} was 0.170 W^2 (Table 4).

Patients were generally able to adjust their volitional leg effort to keep the measured work rate close to the target: the mean value of root-mean-square tracking error for work rate, $RMSE_{WR}$, was 0.53 W (Table 4).

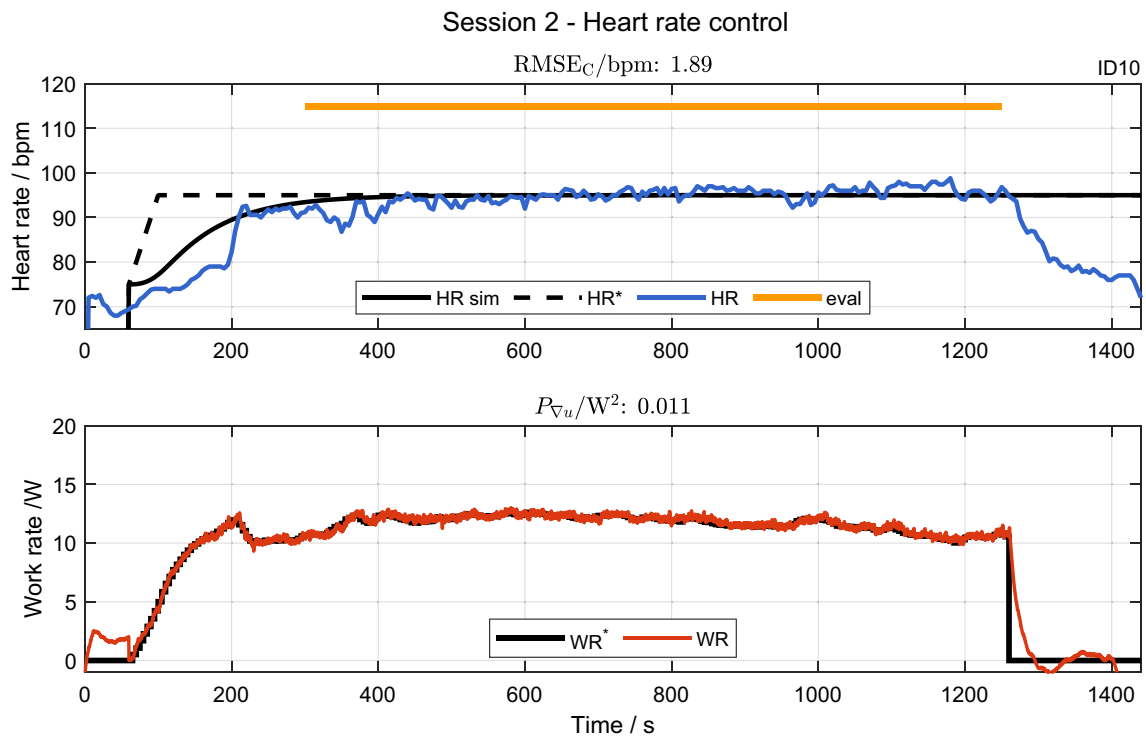
Table 4 Outcome measures for feedback control tests

ID	$RMSE_C$ [bpm]	P_{Vu} [W^2]	$RMSE_{WR}$ [W]
1	1.33	0.016	0.16
2	1.44	0.183	0.35
3	1.36	0.027	0.46
4	1.16	0.013	0.31
5	0.97	0.040	0.44
6	2.90	0.697	0.58
7	4.43	0.234	1.25
8	4.16	0.228	0.43
9	1.97	0.354	0.67
10	1.89	0.011	0.22
11	1.22	0.046	0.71
12	1.17	0.193	0.77
Mean \pm SD	2.00 \pm 1.19	0.170 \pm 0.201	0.53 \pm 0.30

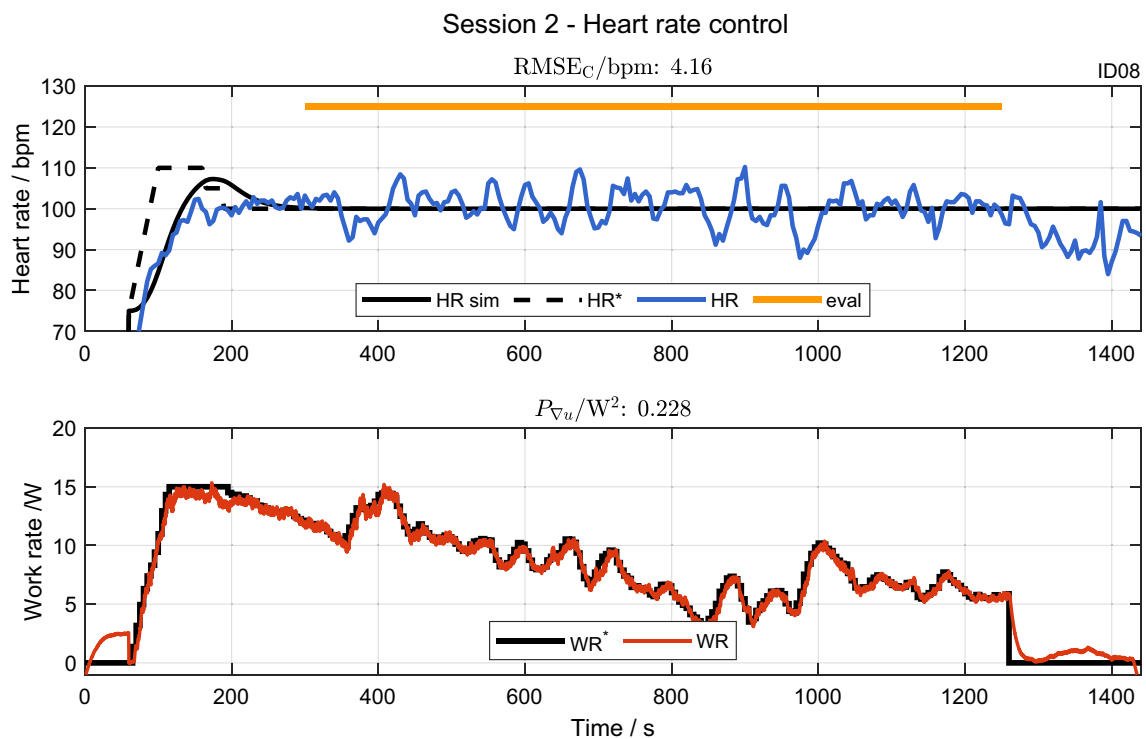
ID: patient identification number; SD: standard deviation

Two exemplary data sets from the feedback control tests, from patients 8 and 10, are provided for illustration (Fig. 10). The test for patient 10 was chosen because the RMS tracking error of 1.89 bpm is closest to the mean $RMSE_C$ for all patients who had P_{Vu} less than the mean value of this outcome variable (Table 4). The test for patient 8 was chosen because, firstly, this patient’s system identification test was used for illustration above (Figs. 8 and 9) and, secondly, because this control test has one of the highest RMS tracking errors, i.e. 4.16 bpm. Inclusion of this test thus provides a degree of empirical evidence of control system robustness.

For patient 10 (Fig. 10a), after the initial transient phase in the first five minutes, HR remained close to the target (upper plot). The control signal, i.e. the target work rate WR^* , is seen to be very smooth (lower plot): in fact,



(a) Patient 10.



(b) Patient 8.

Fig. 10 Feedback control tests for patients 10 and 8. The upper plots show the measured HR (blue), the simulated HR (black, continuous) and the target HR (black, dashed). The lower plots show the target (WR*, black) and actual (WR, red) work rates. The orange bars signify the time periods used for outcome evaluation

this patient had the lowest average control signal power of all tests ($P_{\nabla u} = 0.011 \text{ W}^2$, Table 4). There is some evidence from about time $t = 600 \text{ s}$ onwards of a gradual reduction in work rate, presumably due to the feedback automatically compensating for the cardiovascular drift resulting from fatigue and other factors that is typically seen during prolonged exercise [16]. It is evident from the lower plot in Fig. 10a that this patient was able to follow the target work rate very precisely by continuous modification of their volitional effort: root-mean-square tracking error for work rate, RMSE_{WR} , was 0.22 W , which was the second-lowest value across all patients (Table 4).

For patient 8 (Fig. 10b), HR varies quite widely, but remains on average at the correct target level. There is clear evidence in this test of fatigue onset: target work rate reduces substantially over the course of the test.

Discussion

The aim of this study was to investigate the feasibility of heart rate control during robotics-assisted tilt table exercise in a case series of patients after a stroke.

Feedback control tests were successfully conducted in all 12 patients. Control accuracy was generally very high with a very low mean RMS tracking error, RMSE_C , of just 2.00 bpm , which in relative terms is an error of 2.1% since the mean heart rate was 94 bpm .

Three patients (6, 7 and 8) had RMSE_C values greater than 2 bpm (Table 4), likely due to their relatively high magnitude of heart rate variability (see ref. [17] for a separate analysis of HRV in this study cohort, where HRV magnitude was measured in exercise and resting conditions). Correspondingly, average control signal power

$P_{\nabla u}$ for these patients was also relatively high (Table 4). High RMSE_C and $P_{\nabla u}$ values are a consequence of HRV acting as the principal disturbance entering the feedback control loop (Fig. 6). As discussed in the Results, patient 7 also had difficulty generating enough power to follow the target work rate, thus contributing further to the high RMSE_C and $P_{\nabla u}$ outcomes in this case (Table 4).

Insight into the dependence of the primary outcomes RMSE_C and $P_{\nabla u}$ on the magnitude of HRV can be gleaned by formal analysis of the correlations between these variables. It was found that there was a strong positive correlation between the total power (TP) frequency domain HRV metric (denoted HRV-TP) and RMSE_C , when considering both exercise TP [correlation coefficient $r = 0.84$ ($p = 0.0011$), Fig. 11a] and resting TP [$r = 0.89$ ($p = 0.00026$), Fig. 11b]. On the other hand, there was only moderate correlation between exercise TP and $P_{\nabla u}$ [$r = 0.54$ ($p = 0.083$), Fig. 12a] and weak correlation between resting TP and $P_{\nabla u}$ ($r = 0.33$ [$p = 0.33$], Fig. 12b). This relatively low dependence of average control signal power $P_{\nabla u}$ on HRV magnitude is likely a consequence of the feedback design strategy that purposely specified a low-pass input-sensitivity function [Eq. (5), Sect. "Feedback control"], thus making the control signal u insensitive to HRV at frequencies above the selected bandwidth p .

Note that patients 6 and 8, i.e. those with relatively high RMSE_C values, are highlighted in Figs. 11 and 12. Patient 7 was excluded from the correlation analysis because their HRV magnitudes rendered them an outlier: their TP values were 3030 ms^2 and $11\,864 \text{ ms}^2$ in the exercise and resting conditions, respectively [17] (cf. values for

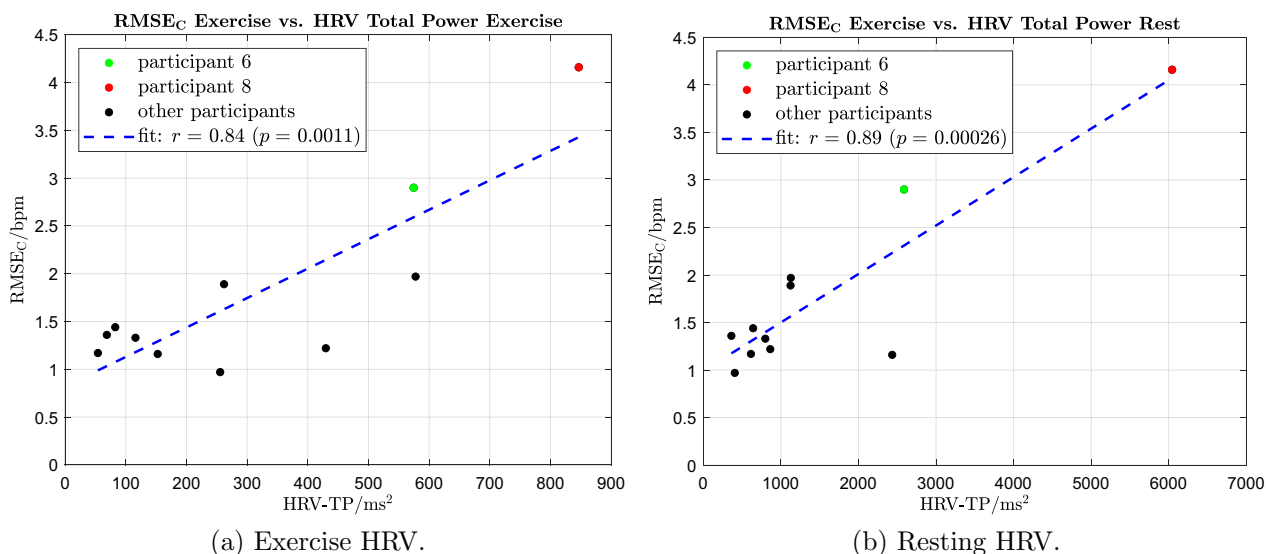


Fig. 11 Correlations between HRV total power magnitude HRV-TP and RMS tracking error RMSE_C

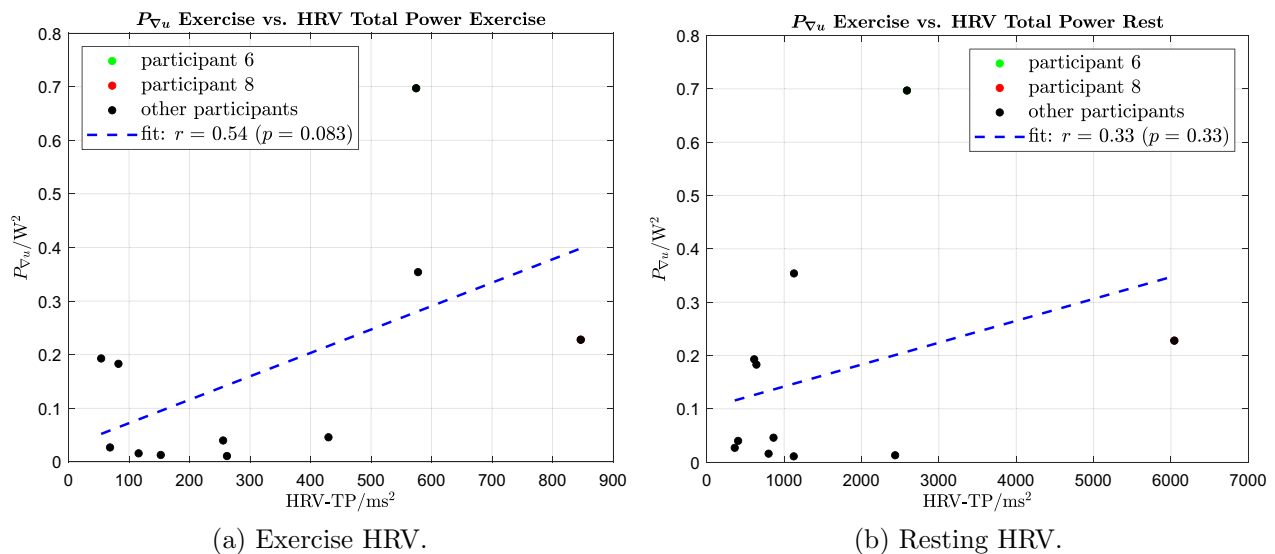


Fig. 12 Correlations between HRV total power magnitude HRV-TP and average control signal power P_{V_u}

other patients in Figs. 11 and 12). These extreme TP values are approximately 3 standard deviations away from their respective means (for exercise TP, the factor was 3.0; for resting TP, the factor was 2.8).

Feedback controllers were calculated individually for each patient based on the system identification tests that provided estimates of dynamic models of heart rate response to changes in exercise work rate. Model parameters were successfully estimated in 11 of 12 patients with a mean RMS model error of 2.00 bpm and fit of 47.2 % for these 11 (excluding RMS error and fit for patient 7 in Table 3). Although patient 7 completed the system identification test, the estimation algorithm failed to deliver plausible values for k and τ , again likely due to this patient's difficulty in maintaining the target work rate and their high level of HRV, leading to low quality input–output data.

From a clinical deployment perspective, it would be desirable not to have to perform individual system identification tests for every patient and to then calculate individual feedback controller parameters. The question thus arises as to whether a single nominal model, taken as an average over multiple patients, could be used to generate a single feedback controller that would provide accurate and robust performance for further patients who did not take part in system identification tests. The quite narrow bounds (95 % CIs) obtained for the mean k and τ parameters, Fig. 7, suggest that such an approach may be feasible. Furthermore, there have been multiple studies using treadmill and cycle ergometer exercise with able-bodied participants. These have demonstrated that a single feedback controller for heart rate, computed from an average

linear time-invariant nominal model of the form Eq. (1), can provide highly accurate and robust performance when applied to participants whose individual dynamic model parameters are not known. This is despite the fact that considerable variation was present in the individual parameters used to compute the nominal model [13]. Further investigation is required to test controller robustness in the context of robotics-assisted exercise in patients with neurological deficits.

A prerequisite for identification and control tests is the ability of the patient to perform volitional control of work rate by focusing on the target and actual values on the biofeedback screen. All patients rapidly understood this cognitive task and, in the feedback control tests, they were able to accurately follow the target work rate with an RMS tracking error of 0.53 W on average. The incorporation of visual feedback within the heart rate control setup, which is a challenging and stimulating cognitive task for the active processing networks of the central nervous system, may bring side benefits: studies that used visual feedback during treadmill-based gait rehabilitation showed positive effects on training outcomes in different cohorts, e.g. cerebral palsy, stroke or Parkinson's disease, i.e. reduction in gait asymmetry, increased mobility [18] and improved balance [19, 20].

An important element of the study design was our choice of a commercially available, medically certified rehabilitation platform that is already widely deployed in clinical settings, namely the Erigo robotics-assisted tilt table. Our approach was to extend the functionality of an established system by the addition of visual work rate feedback, supported by the integration of

leg-force sensors, to facilitate the implementation of physiological training and testing programmes, [5–7], and, in the present study, feedback control of heart rate. We have taken a similar approach in the context of robotics-assisted gait rehabilitation, e.g. using both exoskeleton [21, 22] and end-effector [23, 24] based systems. This approach underscores the importance of integrating cognitive biofeedback and promoting active patient participation in robotics-assisted rehabilitation therapies.

Other investigators have also investigated heart rate control using exoskeleton-type gait robots [25]. In that work, however, only treadmill speed, guidance force, and body weight support level were employed to influence HR. Since the three healthy participants remained passive, only a very limited HR response of 80 bpm \pm 10 bpm was demonstrated.

A limitation of the robotics-assisted tilt table as an exercise modality is that relatively low power can be generated by the legs alone, with a correspondingly low magnitude of heart rate response. This is due in part to the Erigo's maximal cadence of 80 steps/min which is perceived to be slow, and which means that the force needed for a given work rate is relatively high; conversely, a lower force would be required if the cadence could be increased beyond this limit. In terms of magnitude of cardiopulmonary response, it would also be desirable to increase total work rate by the integration of the arms in the exercise.

The parameters of the patient-specific dynamic HR models were obtained at one specific tilt angle and stepping cadence, but the model parameters would be expected to change when different device settings are used. The extent to which this is so, and the consequent effect on HR control performance, should be investigated in future work. Furthermore, it is important in future work to develop guidelines that could be used to specify target HR tracking accuracy from a physiological perspective so that patient-independent controller performance can be assessed.

This study included a diverse cohort of patients with stroke spanning a wide age range and exhibiting varying levels of stroke-related gait impairments, but a limitation of our research pertains to the potential bias introduced by the exclusion criteria. Specifically, we excluded patients with severe cognitive impairment, atrial fibrillation, myocardial infarction, and those who were concurrently prescribed medications known to modulate heart rate response to exercise, such as beta-blockers: this may have resulted in the inclusion of generally healthier patients, potentially limiting the generalisability of the results.

Conclusions

Feedback control of heart rate during robotics-assisted tilt table exercise was found to be feasible in patients with neurological impairments following stroke. Future work should investigate robustness aspects of the feedback control system. Modifications to the exercise modality, or alternative modalities, should be explored that allow higher levels of work rate and heart rate intensity to be achieved.

Abbreviations

ABI	Acquired brain injury
BMI	Body mass index
EKNZ	Ethics Committee of Northwestern and Central Switzerland
FAC	Functional Ambulation Category
FES	Functional electrical stimulation
HR	Heart rate
HRV	Heart rate variability
ID	Patient identification number
MRS	Modified Rankin Scale
NDC	Neurological day centre
NIHSS	National Institutes of Health Stroke Scale
NRMSE	Normalised root-mean-square error
OH	Orthostatic hypotension
RMS	Root-mean-square
RMSE	Root-mean-square error
SCI	Spinal cord injury
SD	Standard deviation
TP	Total power
WR	Work rate

Acknowledgements

Not applicable.

Author contributions

All authors made substantial contributions to the conception and design of the study; LB and JS did the data acquisition; LB and KH performed the data analysis; all authors contributed to the interpretation of the data. KH, LB and JS drafted the manuscript; CS reviewed it critically for important intellectual content. All authors read and approved the final manuscript.

Funding

This work was supported by the Swiss National Science Foundation (Principal Investigator KH, Grant Ref. 320030-185351).

Availability of data and materials

The datasets generated and analysed during the current study are available in the OLOS repository, <https://doi.org/10.34914/olos:jqtxsvbcbllfuro4olbhlN6a> (reserved persistent web link to datasets).

Declarations

Ethics approval and consent to participate

This research was performed in accordance with the Declaration of Helsinki. The study was reviewed and approved by the Ethics Committee of Northwestern and Central Switzerland (EKNZ, Ref. 2022-01935). Patients provided written, informed consent prior to inclusion in the study.

Consent for publication

Not applicable.

Competing interests

The authors declare that they have no competing interests.

Author details

¹rehaLab—the Laboratory for Rehabilitation Engineering, Institute for Human Centred Engineering HuCE, School of Engineering and Computer Science, Bern University of Applied Sciences, 2501 Biel, Switzerland. ²Department of Rehabilitation Medicine, Faculty of Medicine and North-Eastern Stroke Research Group, Khon Kaen University, Khon Kaen, Thailand. ³Research Department, Reha Rheinfelden, 4310 Rheinfelden, Switzerland. ⁴Department of Sport, Exercise and Health, University of Basel, 4052 Basel, Switzerland.

Received: 15 November 2023 Accepted: 7 August 2024

Published online: 12 August 2024

References

- Kim MJ, Farrell J. Orthostatic hypotension: a practical approach. *Am Fam Phys.* 2022;105(1):39–49.
- Kuznetsov AN, Rybalko NV, Daminov VD, Luft AR. Early poststroke rehabilitation using a robotic tilt-table stepper and functional electrical stimulation. *Stroke Res Treat.* 2013;2013: 946056.
- Geiger DE, Behrendt F, Schuster-Amft C. EMG muscle activation pattern of four lower extremity muscles during stair climbing, motor imagery, and robot-assisted stepping: a cross-sectional study in healthy individuals. *BioMed Res Int.* 2019;2019:9351689.
- Bichsel L, Sommer M, Hunt KJ. Entwicklung eines Biofeedback-Systems zur Regelung der Leistung, Herzrate und Sauerstoffaufnahme für robotische Kippstisch-Therapie. *Automatisierungstechnik.* 2011;59(10):622–8 (In German).
- Saengsuwan J, Huber C, Schreiber J, Schuster-Amft C, Nef T, Hunt KJ. Feasibility of cardiopulmonary exercise testing using a robotics-assisted tilt table in dependent-ambulatory stroke patients. *J Neuroeng Rehabil.* 2015;12:88. <https://doi.org/10.1186/s12984-015-0078-5>.
- Saengsuwan J, Berger L, Schuster-Amft C, Nef T, Hunt KJ. Test-retest reliability and four-week changes in cardiopulmonary fitness in stroke patients: evaluation using a robotics-assisted tilt table. *BMC Neurol.* 2016;16:163. <https://doi.org/10.1186/s12883-016-0686-0>.
- Laubacher M, Perret C, Hunt KJ. Work-rate-guided exercise testing in patients with incomplete spinal cord injury using a robotics-assisted tilt-table. *Disabil Rehabil Assist Technol.* 2015;10(5):433–8. <https://doi.org/10.3109/17483107.2014.908246>.
- Tafreshi AS, Klamroth-Marganska V, Nussbaumer S, Riener R. Real-time closed-loop control of human heart rate and blood pressure. *IEEE Trans Biomed Eng.* 2015;62(5):1434–42.
- Paolucci S, Di Vita A, Massicci R, Traballesi M, Bureca I, Matano A, et al. Impact of participation on rehabilitation results: a multivariate study. *Eur J Phys Rehabil Med.* 2012;48(3):455–66.
- Riebe D, Ehrman JK, Liguori G, Magal M, editors. ACSM's guidelines for exercise testing and prescription. 10th ed. Philadelphia: Wolters Kluwer; 2018.
- Julious SA. Sample size of 12 per group rule of thumb for a pilot study. *Pharm Stat.* 2005;4(4):287–91.
- Ljung L. *System identification: theory for the user.* 2nd ed. Upper Saddle River: Prentice Hall; 1998.
- Hunt KJ, Zahnd A, Grunder R. A unified heart rate control approach for cycle ergometer and treadmill exercise. *Biomed Signal Process Control.* 2019. <https://doi.org/10.1016/j.bspc.2019.101601>.
- Åström KJ, Murray RM. *Feedback systems.* Princeton, Oxford: Princeton University Press; 2008.
- Hunt KJ, Fankhauser SE. Heart rate control during treadmill exercise using input-sensitivity shaping for disturbance rejection of very-low-frequency heart rate variability. *Biomed Signal Process Control.* 2016;30:31–42. <https://doi.org/10.1016/j.bspc.2016.06.005>.
- Wingo JE, Ganio MS, Cureton KJ. Cardiovascular drift during heat stress: implications for exercise prescription. *Exerc Sport Sci Rev.* 2012;40(2):88–94.
- Saengsuwan J, Brockmann L, Schuster-Amft C, Hunt KJ. Changes in heart rate variability at rest and during exercise in patients after a stroke: a feasibility study. In preparation. 2024.
- Liu LY, Sangani S, Patterson KK, Fung J, Lamontagne A. Real-time avatar-based feedback to enhance the symmetry of spatiotemporal parameters after stroke: instantaneous effects of different avatar views. *IEEE Trans Neural Syst Rehabil Eng.* 2020;28(4):878–87.
- Almeida QJ, Bhatt H. A manipulation of visual feedback during gait training in Parkinson's disease. *Parkinson's Dis.* 2012;2012:1–7.
- Levin I, Lewek MD, Feasel J, Thorpe DE. Gait training with visual feedback and proprioceptive input to reduce gait asymmetry in adults with cerebral palsy: a case series. *Pediatr Phys Ther.* 2017;29(2):138–45.
- Schindelholz M, Hunt KJ. Feedback control of heart rate during robotics-assisted treadmill exercise. *Technol Health Care.* 2012;20(3):179–94. <https://doi.org/10.3233/THC-2012-0668>.
- Stoller O, de Bruin ED, Schindelholz M, Schuster-Amft C, de Bie RA, Hunt KJ. Efficacy of feedback-controlled robotics-assisted treadmill exercise to improve cardiovascular fitness early after stroke: a randomised controlled pilot trial. *J Neurol Phys Ther.* 2015;39:156–65. <https://doi.org/10.1097/NPT.0000000000000095>.
- Stoller O, Schindelholz M, Hunt KJ. Robot-assisted end-effector-based stair climbing for cardiopulmonary exercise testing: feasibility, reliability and repeatability. *PLoS ONE.* 2016;11(2): e0148932. <https://doi.org/10.1371/journal.pone.0148932>.
- Riedo J, Hunt KJ. Feedback control of heart rate during robotics-assisted end-effector-based stair climbing. *Syst Sci Control Eng.* 2016;4(1):223–34. <https://doi.org/10.1080/21642583.2016.1228487>.
- Koenig A, Caruso A, Bolliger M, Somaini L, Omlin X, Morari M, et al. Model-based heart rate control during robot-assisted gait training. In: *Proc IEEE Int Conf Robotics Automation Shanghai, China; 2011.* p. 4151–6.

Publisher's Note

Springer Nature remains neutral with regard to jurisdictional claims in published maps and institutional affiliations.

Lars Brockmann is a research assistant in the rehaLab.

Jittima Saengsuwan is a research assistant in the rehaLab. JS is also a medical doctor with specialisation in rehabilitation medicine at the Department of Rehabilitation Medicine within Srinagarind Hospital and the Faculty of Medicine at Khon Kaen University, Thailand.

Corina Schuster-Amft is Head of the Research Department at the neurorehabilitation clinic Reha Rheinfelden.

Kenneth J. Hunt is Head of the rehaLab—the Laboratory for Rehabilitation Engineering, part of the Institute for Human Centred Engineering—in the School of Engineering and Computer Science at Bern University of Applied Sciences.